

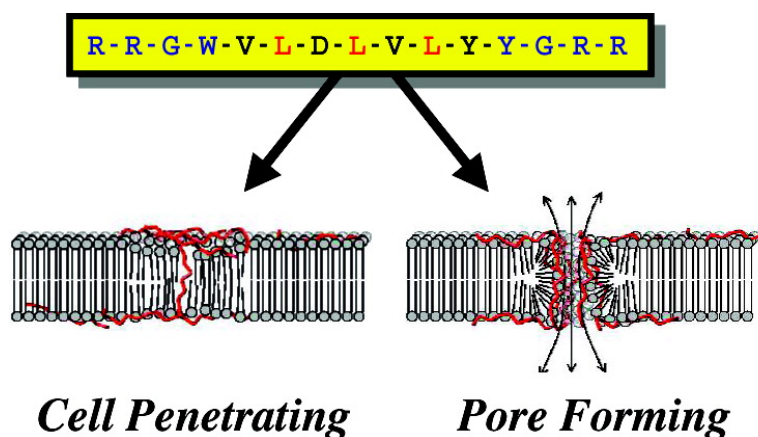
Article

## Biomolecular Engineering by Combinatorial Design and High-Throughput Screening: Small, Soluble Peptides That Permeabilize Membranes

Ramesh Rathinakumar, and William C. Wimley

*J. Am. Chem. Soc.*, **2008**, 130 (30), 9849-9858 • DOI: 10.1021/ja8017863 • Publication Date (Web): 09 July 2008

Downloaded from <http://pubs.acs.org> on February 8, 2009



### More About This Article

Additional resources and features associated with this article are available within the HTML version:

- Supporting Information
- Access to high resolution figures
- Links to articles and content related to this article
- Copyright permission to reproduce figures and/or text from this article

[View the Full Text HTML](#)

## Biomolecular Engineering by Combinatorial Design and High-Throughput Screening: Small, Soluble Peptides That Permeabilize Membranes

Ramesh Rathinakumar and William C. Wimley\*

Department of Biochemistry SL43, Tulane University Health Sciences Center,  
New Orleans, Louisiana 70112-2699

Received March 10, 2008; E-mail: wwimley@tulane.edu

**Abstract:** Rational design and engineering of membrane-active peptides remains a largely unsatisfied goal. We have hypothesized that this is due, in part, to the fact that some membrane activities, such as permeabilization, are not dependent on specific amino acid sequences or specific three-dimensional peptide structures. Instead they depend on interfacial activity: the ability of a molecule to partition into the membrane–water interface and to alter the packing and organization of lipids. Here we test that idea by taking a nonclassical approach to biomolecular engineering and design of membrane-active peptides. A 16 384-member rational combinatorial peptide library, containing peptides of 9–15 amino acids in length, was screened for soluble members that permeabilize phospholipid membranes. A stringent, two-phase, high-throughput screen was used to identify 10 unique peptides that had potent membrane-permeabilizing activity but were also water soluble. These rare and uniquely active peptides do not share any particular sequence motif, peptide length, or net charge, but instead they share common compositional features, secondary structure, and core hydrophobicity. We show that they function by a common mechanism that depends mostly on interfacial activity and leads to transient pore formation. We demonstrate here that composition–space peptide libraries coupled with function-based high-throughput screens can lead to the discovery of diverse, soluble, and highly potent membrane-permeabilizing peptides.

### Introduction

Designing and engineering polypeptides that have specific structures or functions in biological membranes remains one of the more intractable problems in bioengineering. Although the general principles of binding, folding, and self-assembly in membranes are well known,<sup>1,2</sup> the details are not understood well enough for rational *de novo* design. Furthermore, examples of membrane protein structures are also relatively uncommon, and the known examples lack the high diversity of structural classes that would be useful for homology-based or templated design.

One desirable bioengineering objective that could lead to new biosensors, antibiotics, and cell-penetrating peptides is the design of polypeptides that destabilize the permeability barrier of lipid bilayer membranes. For this reason, a great deal of effort has been put into trying to understand the structure–function relationships of known membrane-destabilizing peptides, and some attempts at rational design have been reported.<sup>3–5</sup> Despite a vast literature, compelling structure–function relationships in

this field are very rare. Instead, recent literature suggests strongly that some important functions of peptides in biological membranes, such as pore formation,<sup>6–8</sup> antimicrobial activity,<sup>6,9–12</sup> or membrane translocation of some peptides and attached cargo molecules,<sup>13–16</sup> are not dependent on specific amino acid sequences or three-dimensional peptide structures. Instead they depend on interfacial activity, which is defined here as the ability of a molecule to partition into the membrane–water interface and to alter or strain the packing and organization of the lipids. Interfacial activity depends mainly on the appropriate balance of physical–chemical interactions between and among peptides,

- (1) White, S. H.; Wimley, W. C. *Annu. Rev. Biophys. Biomol. Struct.* **1999**, *28*, 319–365.
- (2) White, S. H.; Wimley, W. C. *Biochim. Biophys. Acta* **1998**, *1376*, 339–352.
- (3) Nguyen, L. T.; Schibli, D. J.; Vogel, H. J. *J. Pept. Sci.* **2005**, *11*, 379–389.
- (4) Kondejewski, L. H.; Jelokhani-Niaraki, M.; Farmer, S. W.; Lix, B.; Kay, C. M.; Sykes, B. D.; Hancock, R. E.; Hodges, R. S. *J. Biol. Chem.* **1999**, *274*, 13181–13192.
- (5) Shai, Y.; Oren, Z. *Peptides* **2001**, *22*, 1629–1641.

- (6) Jin, Y.; Hammer, J.; Pate, M.; Zhang, Y.; Zhu, F.; Zmuda, E.; Blazyk, J. *Antimicrob. Agents Chemother.* **2005**, *49*, 4957–4964.
- (7) Rausch, J. M.; Marks, J. R.; Wimley, W. C. *Proc. Natl. Acad. Sci. U.S.A.* **2005**, *102*, 10511–10515.
- (8) Papo, N.; Shai, Y. *Biochemistry* **2004**, *43*, 6393–6403.
- (9) Rausch, J. M.; Marks, J. R.; Rathinakumar, R.; Wimley, W. C. *Biochemistry* **2007**, *46*, 12124–12139.
- (10) Hilpert, K.; Elliott, M. R.; Volkmer-Engert, R.; Henklein, P.; Donini, O.; Zhou, Q.; Winkler, D. F.; Hancock, R. E. *Chem. Biol.* **2006**, *13*, 1101–1107.
- (11) Hilpert, K.; Volkmer-Engert, R.; Walter, T.; Hancock, R. E. *Nat. Biotechnol.* **2005**, *23*, 1008–1012.
- (12) Mowery, B. P.; Lee, S. E.; Kissounko, D. A.; Eband, R. F.; Eband, R. M.; Weisblum, B.; Stahl, S. S.; Gellman, S. H. *J. Am. Chem. Soc.* **2007**, *129*, 15474–15476.
- (13) Magzoub, M.; Oglecka, K.; Pramanik, A.; Goran Eriksson, L. E.; Graslund, A. *Biochim. Biophys. Acta* **2005**, *1716*, 126–136.
- (14) Magzoub, M.; Pramanik, A.; Graslund, A. *Biochemistry* **2005**, *44*, 14890–14897.
- (15) Potocky, T. B.; Silvius, J.; Menon, A. K.; Gellman, S. H. *ChemBioChem* **2007**, *8*, 917–926.
- (16) Joliot, A.; Prochiantz, A. *Nat. Cell Biol.* **2004**, *6*, 189–196.

water, and membrane lipids, which depend more on the amino acid composition of a peptide than on its exact sequence.<sup>17</sup>

The hundreds of known membrane-active, antimicrobial peptides (AMPs) provide many good examples in which specific sequences or three-dimensional structures are apparently not required for their biological activity.<sup>6,9–12</sup> Growing evidence suggests that some cell-penetrating peptides may function by a similarly nonspecific mechanism.<sup>18</sup> The activity of such molecules *in vitro* and *in vivo* depends on their propensity to bind to membranes and self-assemble into peptide–lipid domains that alter membrane permeability. For AMPs, this hypothesis explains why compelling structure–activity relationships are so difficult to find. For example, Hancock and colleagues<sup>10</sup> made 50 randomly scrambled sequence variants of a potent 12-residue, membrane-permeabilizing AMP named Bac2A. They found that about 50% of the scrambled sequences had antimicrobial activity that was at least as good as that of the parent compound, and 20% of the scrambled sequences had activity that was better than that of the parent peptide. Upon further analysis, these authors concluded, “Sequence alignments of the scrambled Bac2A peptides failed to demonstrate any correlation between peptide sequence and activity.”<sup>10</sup> Subsequent QSAR analysis revealed several broad features that correlate with activity, including having a “hydrophobic patch” anywhere in the molecule and having a certain distance between cationic residues. These vague descriptors relate mostly to global hydrophobicity and thus are consistent with the idea that physical, chemical, and interfacial properties are the critical factors for determining the biological activity of membrane-stabilizing peptides. Other studies in the literature, including our own work, strongly support this idea.<sup>3,6,8,12,19–24</sup> On the basis of this alternative view of peptide function in membranes, we hypothesize that structure-based rational design of membrane-active peptides will not be effective and that potent pore-forming peptides might be more effectively selected from libraries that vary a peptides *composition* instead of peptides or libraries designed with a particular *structure* in mind. In this work, we test the hypothesis and find results that support it.

The interfacial activity of membrane-destabilizing peptides is recapitulated in synthetic bilayer vesicles,<sup>7,23,24</sup> which can thus serve as model systems for membrane-permeabilizing and membrane-translocating peptides. We have previously used such model systems in a structure-based approach to find pore-forming peptides.<sup>7,9</sup> Here we take a nonclassical approach to biomolecular engineering and design of membrane-active peptides by using libraries with rationally designed *composition* coupled with a function-based screening method. We have designed compositionally constrained, combinatorial peptide libraries to select peptides that are small and soluble, but which also bind to membranes and induce membrane permeability at low peptide concentration. We describe here the characteristics of the potent pore-formers selected from this library and detail their mechanism of action in synthetic phospholipid bilayers.

Although they share little sequence similarity in variable positions, the most active molecules share physical properties such as hydrophobicity, and they share the same secondary structure and mechanism of action. The observed mechanism is entirely consistent with having its basis in non-sequence-specific interfacial activity. This information leads us to propose a new general model for the mechanism of action of these peptides in membranes. We show here that composition–space peptide libraries coupled with function-based high-throughput screens can lead to the discovery of diverse, soluble, and potentially membrane-active peptides.

## Materials and Methods

**Reagents.** Most chemicals and materials were purchased through Fischer Scientific (St. Louis, MO) and Sigma-Aldrich (St. Louis, MO). Tentagel macrobeads and Tentagel S resin were obtained from RAPP Polymere (Tubingen, Germany). Fmoc-photolabile linker, Fmoc-amino acids, and all other peptide synthesis reagents were obtained from Advanced Chemtech (Louisville, KY). TbCl<sub>3</sub>, dipicolinic acid (DPA), 8-aminonaphthalene-1,3,6-trisulfonic acid (ANTS), *p*-xylene-bis-pyridinium bromide (DPX), and 3 and 40 kDa fluorescein-labeled dextran were purchased from Molecular Probes (Eugene, OR).

**Combinatorial Peptide Library Synthesis.** The combinatorial peptide library was synthesized on Tentagel NH<sub>2</sub> macrobeads of 50–60 mesh pore size (80 000 beads per gram) using a combination of manual and automated syntheses with an Applied Biosystems Pioneer synthesizer (Foster City, CA), as described previously.<sup>7,9</sup> Active amino groups on the macrobeads were first acylated with photolabile linker, followed by peptide synthesis. Combinatorial sites were synthesized by the split-and-pool method.<sup>9,25</sup> Side-chain protecting groups were removed by Reagent R (90% (v/v) trifluoroacetic acid, 5% thioanisole, 3% ethanedithiol, and 2% anisole). Residual Reagent R solution was drained, and beads were washed multiple times with dichloromethane and dried under a nitrogen gas stream in a fume hood.

**Peptide Synthesis.** Bulk peptide synthesis was carried out using Tentagel SAM peptide amide resin (0.2 mmol/g) on an Applied Biosystems Pioneer synthesizer by standard Fmoc solid-phase peptide synthesis methods,<sup>26,27</sup> as described in detail elsewhere.<sup>7,9</sup> The identity of the purified peptides was confirmed by MALDI mass spectroscopy.

**Liposome Preparation.** Large unilamellar vesicles (LUVs) of 0.1 μm diameter were prepared by extrusion.<sup>28</sup> Lipids were dried from chloroform and rehydrated with buffer to a concentration of 100 mM lipid to maximize encapsulation. The lipid solution was subjected to least 20 repeated freeze–thaw cycles. For Tb<sup>3+</sup> encapsulated in LUVs, a resuspension buffer of 50 mM TbCl<sub>3</sub>, 100 mM sodium citrate, and 10 mM N-Tris-(Hydroxymethyl) methyl-2-aminoethane sulfonic acid (TES) at pH 7.0 was used. ANTS/DPX LUVs were prepared with a resuspension buffer of 25 mM ANTS, 5 mM DPX, and 10 mM potassium phosphate at pH 7.0. For LUVs encapsulating 3 and 40 kDa fluorescein-labeled dextran, a resuspension buffer of 10 mg/mL labeled dextran and 10 mM potassium phosphate, pH 7.0, was used. Following extrusion, LUVs were eluted over a Sephadex G-200 gel filtration column (4 cm i.d., 40 cm length) equilibrated with elution buffer that does not contain probe molecules to separate vesicles from external marker molecules. Lipid concentration was measured using the Bartlett assay.

- (17) Wimley, W. C.; White, S. H. *Nat. Struct. Biol.* **1996**, *3*, 842–848.  
 (18) Magzoub, M.; Eriksson, L. E.; Graslund, A. *Biophys. Chem.* **2003**, *103*, 271–288.  
 (19) Avrahami, D.; Oren, Z.; Shai, Y. *Biochemistry* **2001**, *40*, 12591–12603.  
 (20) Raguse, T. L.; Porter, E. A.; Weisblum, B.; Gellman, S. H. *J. Am. Chem. Soc.* **2002**, *124*, 12774–12785.  
 (21) Oren, Z.; Shai, Y. *Biochemistry* **1997**, *36*, 1826–1835.  
 (22) Shai, Y.; Oren, Z. *J. Biol. Chem.* **1996**, *271*, 7305–7308.  
 (23) White, S. H.; Wimley, W. C.; Selsted, M. E. *Cur. Opin. Struct. Biol.* **1995**, *5*, 521–527.  
 (24) Wimley, W. C.; Selsted, M. E.; White, S. H. *Protein Sci.* **1994**, *3*, 1362–1373.

- (25) Lam, K. S.; Lehman, A. L.; Song, A.; Doan, N.; Enstrom, A. M.; Maxwell, J.; Liu, R. *Methods Enzymol.* **2003**, *369*, 298–322.  
 (26) Grant, G. A. *Synthetic Peptides: A User's Guide*; W.H. Freeman and Co.: New York, 1992.  
 (27) Atherton, E.; Sheppard, R. C. *Solid phase peptide synthesis*; IRL Press: Oxford, 1989.  
 (28) Nayar, R.; Hope, M. J.; Cullis, P. R. *Biochim. Biophys. Acta* **1989**, *986*, 200–206.

**High-Throughput Screening Assay.** To prepare a bead-tethered library for screening, beads were spread uniformly in Petri dishes using methanol. After drying completely, the beads were exposed to a long-wavelength UV lamp (365 nm) for 5 h to cleave the peptide from the beads, giving C-terminal amides. Library beads were then separated into individual wells of 96-well plates, and then 10  $\mu\text{L}$  of dry dimethylsulfoxide (DMSO) was added and the plates were incubated overnight to extract the peptides from the beads. Because we have previously found that absorption of atmospheric water into hygroscopic DMSO inhibits peptide release,<sup>7</sup> overnight incubation of plates was done in a desiccator closed under vacuum. Approximately 1–2 nmol of peptide was consistently released from each bead.

The high-throughput screen is based on encapsulation of terbium inside phospholipid vesicles and the addition of the aromatic chelator DPA to the external solution. Formation of the highly luminescent  $\text{Tb}^{3+}$ /DPA complex occurs only when the membranes are permeabilized.<sup>29</sup> For high-throughput screening, the peptides in DMSO were ultimately diluted to 10  $\mu\text{M}$  in each well with an excess of aqueous screening solution containing 500  $\mu\text{M}$  LUVs with  $\text{Tb}^{3+}$  encapsulated and 50  $\mu\text{M}$  external DPA. The typical lipid composition of LUVs was 90% zwitterionic 1-palmitoyl-2-oleoyl-*sn*-glycero-3-phosphatidylcholine (POPC) and 10% anionic 1-palmitoyl-2-oleoyl-*sn*-glycero-3-phosphatidylglycerol (POPG). We tested two orders of addition. In the “direct mixing” strategy, the screening assay solution of LUVs and DPA was added directly to the library peptides, extracted from the beads into 10  $\mu\text{L}$  of DMSO, allowing for immediate interaction of peptides with membranes. In the “premixing” strategy, we mixed the peptides in DMSO with buffer alone and incubated that solution for a minimum of 30 min to allow insoluble peptides to precipitate. Later, the screening solution containing LUV and DPA was added and incubated for another 45 min. We observed about 3-fold more active peptides by using the direct mixing strategy, indicating that many active peptides are also insoluble. Because soluble peptides are more useful and amenable to further mechanistic studies, we screened the library using the premixing strategy at a peptide-to-lipid ratio of approximately 1:50. The screening plates were visualized and photographed under short-wave UV light in a darkroom, and wells with the brightest  $\text{Tb}^{3+}$ /DPA luminescence were selected as positive for pore formation. The beads from those wells were sent to Kansas State University Biotech core laboratories (Manhattan, KS) for sequencing by Edman degradation.

**Circular Dichroism.** Peptides, dissolved in dilute acetic acid stock solutions, were added to 10 mM potassium phosphate buffer, pH 7.0, to bring the concentration to 50  $\mu\text{M}$ . The circular dichroism (CD) spectra were recorded on a Jasco 810 spectropolarimeter (Easton, MD) between 180 and 260 nm using a quartz cuvette with 0.1 cm path length. CD spectra were measured before and after the addition of 2.5 mM LUVs composed of 9:1 POPC:POPG. Spectra were corrected for the buffer background contribution and represented as mean residue ellipticity ( $\Theta$ ).

**Peptide Partitioning.** Peptide partitioning into lipid bilayers was monitored by fluorescence enhancement of tryptophan upon addition of liposomes. Tryptophan fluorescence was measured using excitation at 270 nm and scanning emission between 290 and 510 nm with 8 nm bandwidths on an SLM-Aminco fluorescence spectrophotometer. Emission spectra were measured using 4  $\mu\text{M}$  peptide in 10 mM potassium phosphate buffer, pH 7.0, titrated with LUVs composed of 9:1 POPC:POPG up to a concentration of 1.2 mM lipid. Background and lipid scattering effects were subtracted. For each titration, the fluorescence intensity at 330 nm ( $I$ ) was normalized to the intensity of peptide in buffer ( $I_0$ ). Mole fraction partition coefficients ( $K_x$ ) were obtained by fitting to the equation

$$\frac{I}{I_0} = 1 + (I_{\text{max}} - 1) \left( \frac{K_x[\text{L}]}{K_x[\text{L}] + [\text{W}]} \right)$$

where  $I$  is the fluorescence intensity and  $I_0$  and  $I_{\text{max}}$  are the intensities before lipid addition and after saturation of peptide–lipid binding.  $[\text{L}]$  is the molar lipid concentration, and  $[\text{W}]$  is the molar concentration of water (55.3 M). For any experiment, the fraction of peptide bound can be calculated by

$$\text{fraction bound} = \frac{K_x[\text{L}]}{K_x[\text{L}] + [\text{W}]}$$

Measured partition coefficients were independent of peptide concentration, indicating “infinite dilution” conditions.  $K_x$  is thus a true partition coefficient. However, we note that the contribution of electrostatic interactions to binding is influenced by experimental details such as bilayer surface charge and ionic strength,<sup>30,31</sup> and these partition coefficients are thus specific for our experimental conditions.

**Liposome Leakage Assays.** Four probe sets were used to characterize leakage:  $\text{Tb}^{3+}$ /DPA (see above), ANTS/DPX, an obligate fluorophore/quencher pair, and two labeled dextrans of 3000 and 40 000 g/mol.  $\text{Tb}^{3+}$  leakage was measured by the increase in fluorescence upon formation of the complex  $\text{Tb}^{3+}$ /DPA. The ANTS/DPX assay measures leakage by the relief of quenching of ANTS by co-encapsulated DPX. Fluorescein–dextran leakage was measured by relief of fluorescein self-quenching. Complete release of probes was assessed by Triton-X solubilization of liposomes. Measurements were done at 500  $\mu\text{M}$  lipid concentration and peptide concentrations from 1 to 10  $\mu\text{M}$ , or peptide:lipid (P:L) ratios from 1:500 through 1:50. Peptides in buffer were added to liposomes and mixed using a syringe, followed by 30–60 min of incubation. For all probes, there is a burst of leakage that slows over 15–30 min and ceases completely after about 30 min. Fluorescence emission spectra were measured using excitation/emission wavelengths of 270/490 nm for  $\text{Tb}^{3+}$ /DPA, 350/510 nm for ANTS/DPX, and 490/520 for the dextrans. We varied the order of addition—concentrated peptide into dilute liposomes or concentrated liposomes into dilute peptide—and found no significant difference in the amount of leakage from the vesicles. We also found no effect of preincubation of peptide in buffer before addition of lipid solutions.

The time dependence of leakage of  $\text{Tb}^{3+}$  from LUVs was continuously monitored for 30 min. Peptides were added from a stock solution to 1 mL of assay solution in a quartz cuvette with a rotating stir bar. The assay solution consists of 500  $\mu\text{M}$  LUVs with entrapped  $\text{TbCl}_3$  in 10 mM TES and 300 mM NaCl at pH 7.0, and external DPA at 50  $\mu\text{M}$ . Different P:L ratios were obtained by varying the peptide concentration from 1 to 10  $\mu\text{M}$ . Complete release of  $\text{Tb}^{3+}$  was achieved by adding excess Triton X-100 after 25 min.

**ANTS/DPX Requenching Assay.** The ANTS/DPX requenching assay, described previously,<sup>24,32,33</sup> was used to determine whether the mechanism of leakage induced by the peptides is all-or-none or graded. Here, the peptides in 10 mM potassium phosphate buffer, pH 7.0, were mixed with 500  $\mu\text{M}$  LUVs with entrapped dye ANTS and its quencher DPX. The peptide concentration varied from 1 to 10  $\mu\text{M}$  to attain various P:L ratios, and the leakage was allowed to proceed for 30 min until it had stopped. The quencher DPX was then titrated externally to quench the ANTS that had leaked out. ANTS that remains entrapped inside the LUVs is not quenched by externally added DPX. Complete leakage was obtained by adding Triton X-100. The fraction of ANTS released and the quenching

(30) Montich, G.; Scarlata, S.; McLaughlin, S.; Lehrmann, R.; Seelig, J. *Biochim. Biophys. Acta* **1993**, *1146*, 17–24.

(31) Murray, D.; Hermida-Matsumoto, L.; Buser, C. A.; Tsang, J.; Sigal, C. T.; Ben-Tal, N.; Honig, B.; Resh, M. D.; McLaughlin, S. *Biochemistry* **1998**, *37*, 2145–2159.

(32) Ladokhin, A. S.; Wimley, W. C.; Hristova, K.; White, S. H. *Methods Enzymol.* **1997**, *278*, 474–486.

(33) Ladokhin, A. S.; Wimley, W. C.; White, S. H. *Biophys. J.* **1995**, *69*, 1964–1971.

(29) Rausch, J. M.; Wimley, W. C. *Anal. Biochem.* **2001**, *293*, 258–263.

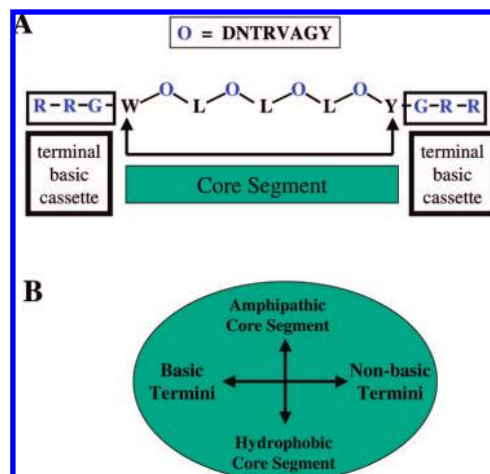


**Figure 1.** Design of the rational combinatorial library used in this work. The core segment of nine residues contains five fixed hydrophobic residues and four (O) that are varied combinatorially as indicated. The core sequences explore a region of compositional space ranging from those which are highly charged and amphipathic, to sequences with a polar–nonpolar dyad repeat sequence like the membrane-spanning strands of  $\beta$ -barrel membrane proteins,<sup>35</sup> to sequences that are totally nonpolar. Independently, the end groups were varied in the library such that the RRG– and –GRR terminal basic cassettes were randomly and independently present or absent in each peptide sequence in the library.

of the ANTS that remains entrapped within the vesicles were calculated as described previously.<sup>24,32,33</sup>

## Results

**Combinatorial Peptide Library Design.** The 16 384-member combinatorial peptide library shown in Figure 1 was designed to probe the sequence/composition requirements for membrane-permeabilizing activity. A core segment length of nine residues was chosen to minimize complexity while encompassing a length similar to the smallest natural membrane-permeabilizing peptides. Two orthogonal compositional variations were used to test the requirements for selecting soluble, potentially membrane-destabilizing peptides. The core nine-residue sequence has five fixed positions, chosen on the basis of their hydrophobicity<sup>17</sup> to ensure that most library members will interact with membranes, and four varied positions, designed specifically to test a broad range of compositions. This library specifically tests the requirement for a strict dyad repeat of alternating polar and nonpolar residues, which are always found in membrane-spanning  $\beta$ -sheet proteins<sup>34–36</sup> and are sometimes, but not always, found in peptide pore-formers.<sup>37–39</sup> The four combinatorial sites were substituted either with one of the polar or charged amino acids threonine, arginine, aspartic acid, or asparagine or with one of the increasingly hydrophobic amino acids glycine, alanine, valine, or tyrosine. Possible core segments in the library thus include highly charged dyad repeats, canonical membrane-spanning  $\beta$ -sheet dyad repeats,<sup>35</sup> and even totally hydrophobic sequences. Tryptophan and tyrosine were placed at the ends of the core sequence to promote membrane binding<sup>40</sup>

and to mimic membrane  $\beta$ -sheets.<sup>35</sup> Aromatic residues, especially tyrosine and tryptophan, are abundantly present at the membrane aqueous bilayer interface of all membrane protein and membrane-active peptides,<sup>37,40</sup> where they contribute strongly to membrane binding.<sup>17,40</sup>

The peptide library was synthesized randomly with or without the Arg–Arg–Gly- or –Gly–Arg–Arg terminal basic cassettes such that each core sequence in the library was present in four forms, one with a basic cassette at the N-terminus, one with the cassette at the C-terminus, one with basic cassettes at both termini, and one with basic cassettes at neither terminus. This was done to modulate the overall solubility and hydrophobicity of the peptides and allow for the selection of more hydrophobic core peptides that would be made soluble by charged terminal segments. The carboxyl terminus is an uncharged carboxamide.

**Screening for Soluble Membrane-Destabilizing Peptides.** To screen the combinatorial library for potent membrane-destabilizing peptides, we used a two-step, high-throughput assay that selects for peptides that are soluble, but which also permeabilize membranes. For this we used a phospholipid vesicle-based high-throughput screen as described above.<sup>7,29</sup> Screening was carried out in two different stages, first selecting against insoluble peptides and then selecting the remaining peptides for membrane permeabilization. In this strategy, which we refer to as “pre-mixing”, the peptides, extracted from synthesis beads with 10  $\mu$ L of dry DMSO, were then incubated with buffer solution for 30 min to several hours before addition of the vesicle assay solution. This facilitates the selection of only monomeric peptides or small soluble aggregates, because insoluble peptide aggregates will come out of solution.

In the high-throughput assays, premixed screens were done at 1:50 P:L, where about 5% of the library caused detectable leakage and about 0.1% of the library members caused significant (> 50%) leakage from the vesicles. Potent membrane-permeabilizing peptides were identified from the intensity of fluorescence. About 20 000 beads were screened from the 16 384 members of the library.<sup>41</sup>

**Selection and Characterization of Membrane-Destabilizing Peptides.** Fourteen peptides were found to have potent membrane-destabilizing activity in the 20 000 beads screened using the premixing strategy. These peptides were identified by Edman sequencing directly from the bead. The amino acid sequences are shown in Figure 2. Importantly, three of these sequences were independently identified more than once, indicating that there is only a very small population of potent peptides and that we have identified most of them. A conserved sequence motif or peptide length did not emerge from the screening and selection process. However, there are some characteristics we can identify. Most of the potent peptides contained a single polar amino acid and three hydrophobic residues in the four varied sites. In 7 of the 10 sequences from the pre-mixing screen, there is a single arginine residue (see Figure 2 and Table 1), while one sequence has aspartate and one has two threonines. Asparagine was not observed in the premixing sequences ( $p = 0.007$ ), and aspartate was observed only once ( $p = 0.04$ ). There is a large excess of valine ( $p = 0.0002$ ), such that 9 of the 10

(34) Wimley, W. C. *Curr. Opin. Struct. Biol.* **2003**, *13*, 404–411.

(35) Wimley, W. C. *Protein Sci.* **2002**, *11*, 301–312.

(36) Schulz, G. E. *Curr. Opin. Struct. Biol.* **2000**, *10*, 443–447.

(37) Yount, N. Y.; Yeaman, M. R. *Proc. Natl. Acad. Sci.* **2004**, *101*, 7363–7368.

(38) Yeaman, M. R.; Yount, N. Y. *Pharmacol. Rev.* **2003**, *55*, 27–55.

(39) Hancock, R. E. W.; Lehrer, R. *Trends Biotechnol.* **1998**, *16*, 82–88.

(40) Yau, W. M.; Wimley, W. C.; Gawrisch, K.; White, S. H. *Biochemistry* **1998**, *37*, 14713–14718.

(41) The probability of screening a particular member of a library  $n$  times,  $P_n$ , can be calculated using the Poisson equation,  $P_n = e^{-\mu}(\mu^n/n!)$ , where  $\mu$  is the number of copies of the library that has been screened overall. In this case,  $\mu = 20000/16384 = 1.25$ . The probability of screening a particular member of the library at least once ( $\sum P_n$  for  $n \neq 0$ ), also known as the library coverage, is 0.72.

R-R-G-W-V-L-D-L-V-L-Y	Y-G-R-R (3)	*VDVY
R-R-G-W-V-L-A-L-V-L-Y	Y-G-R-R (1)	*VAVY
R-R-G-W-V-L-A-L-V-L-R	Y-G-R-R (1)	*VAVR
R-R-G-W-V-L-A-L-Y-L-R	Y-G-R-R (1)	*VAYR
R-R-G-W-V-L-R-L-A-L-A	Y----- (1)	*VRAA
R-R-G-W-A-L-R-L-V-L-A	Y----- (2)	*ARVA
R-R-G-W-R-L-V-L-A-L-V	Y----- (1)	*RVAV
-----W-Y-L-T-L-T-L-G	Y-G-R-R (1)	YTTG
-----W-A-L-R-L-Y-L-V	Y----- (1)	ARYV
-----W-V-L-V-L-R-L-G	Y----- (2)	VVRG

**Figure 2.** Sequences of the soluble potent pore-formers selected. About 20 000 peptides belonging to the 16 384 member library shown in Figure 1 were screened at a 1:50 P:L ratio. The screen included a pre-incubation in buffer to select against insoluble peptides. Fourteen very potent membrane-permeabilizing peptides were identified, and their sequences were determined, giving 10 unique sequences. Three peptides were identified two or three times independently, as indicated by the numbers in parentheses. Shorthand names, at right, contain the identity of the four varied core residues, with asterisks indicating the presence of a terminal basic cassette.

**Table 1.** Statistics of Amino Acid Abundance in Selected Peptides

amino acid	premixed screen <sup>a</sup>	
	occurrence	<i>p</i> -value <sup>b</sup>
D	1	0.040
N	0	0.007
T	2	ns <sup>c</sup>
R	7	ns
V	14	0.0002
A	9	ns
G	2	ns
Y	5	ns

<sup>a</sup> The number of each residue observed in the variable positions in the 10 most potent sequences observed in the premixed screen (see text). Sequences observed multiple times (Figure 2) are counted only once. <sup>b</sup> The probability that the occurrence of that residue is random and the observed number was made by chance. <sup>c</sup> Not significant at the  $p < 0.05$  significance level.

pre-mixing sequences contain at least one valine and 5 of the 10 sequences contain two of them.

To assess the hydrophobicity of the selected core segments, we compared the selected peptides with the whole library using an experimentally measured membrane hydrophobicity scale. In Figure 3, we show a histogram of the Wimley–White hydrophobicity<sup>1,17</sup> of the core segment of the library, with the values of the 10 selected peptides shown as points. The selected peptides are not randomly selected from the parent distribution ( $p < 0.001$ ) and are narrowly clustered ( $p = 0.03$  for width only), suggesting that the selection is dominated by a balance of hydrophilicity (solubility) and hydrophobicity (membrane interaction).

#### Secondary Structure and Peptide–Membrane Interaction.

We synthesized and purified the 10 peptides in Figure 2 for detailed analysis. All 10 peptides were readily water-soluble ( $> 1$  mM in 0.05% HOAc). We used fluorescence enhancement to measure peptide binding, expressed as mole fraction partition coefficients.<sup>42</sup> The peptides in solution were titrated with vesicles composed of 9:1 POPC:POPG, and the tryptophan fluorescence was monitored. Fluorescence intensity increased 2- to 4-fold (Figure 4), and the maximum emission wavelength shifted from 350 nm in buffer to about 332 nm in lipid environment,

(42) White, S. H.; Wimley, W. C.; Ladokhin, A. S.; Hristova, K. *Methods Enzymol.* **1998**, 295, 62–87.

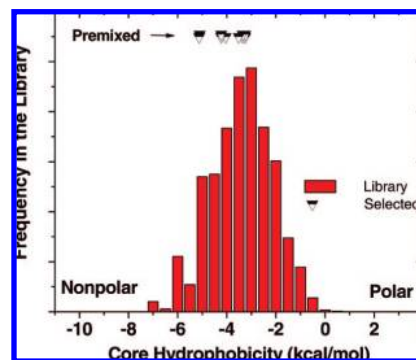


**Figure 3.** Hydrophobicity analysis of the selected peptides. The experimentally determined Wimley–White membrane hydrophobicity score<sup>1,17</sup> was used to show a histogram of membrane hydrophobicity of the core sequence of the whole library. At the top we show the individual scores for the potent membrane-permeabilizing peptides selected (Figure 1). The selected peptides fall into a narrow region on the more hydrophobic side of the library and were not randomly selected from the whole distribution ( $p < 0.001$ ).

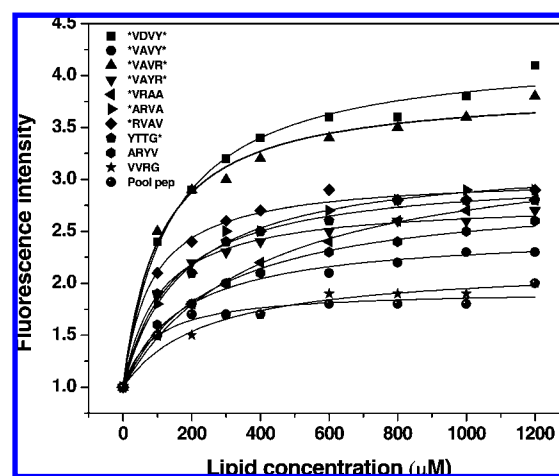


**Figure 4.** Binding isotherms for peptides interacting with lipid bilayer vesicles. The fluorescence intensity of the peptide tryptophan residue at 330 nm was measured as lipid vesicles were titrated into the samples. Samples contained the peptides dissolved in buffer, and measurements were made after addition of aliquots of lipid vesicles containing 90% POPC and 10% POPG. At least 10 min was allowed for equilibration, although steady-state fluorescence was reached within 3–5 min. Mole fraction partition coefficients were calculated as described in the text.

indicating a less polar environment for the Trp residue, consistent with a surface-bound, interfacial environment for the peptide.<sup>43</sup> The mole fraction partition coefficients ( $K_x$ ) ranged narrowly from  $2 \times 10^5$  to  $6 \times 10^5$ . All the selected peptides thus have good membrane binding. In this range of  $K_x$  values, all peptides also have a detectable equilibrium between bound and free peptide. The pooled peptides also showed binding to the vesicles with an apparent partition coefficient that is similar to that of the selected peptides. However, we note that a fluorescence titration experiment in a mixed population gives not an “average” partition coefficient but one that is weighted in favor of those members that do bind. Nonetheless, this measurement shows that the membrane-permeabilizing peptides screened from the library were not selected only on the basis of membrane binding, but rather due to their differences in properties that determine their ability to permeabilize membranes.

(43) Ladokhin, A. S.; Jayasinghe, S.; White, S. H. *Anal. Biochem.* **2000**, 285, 235–245.

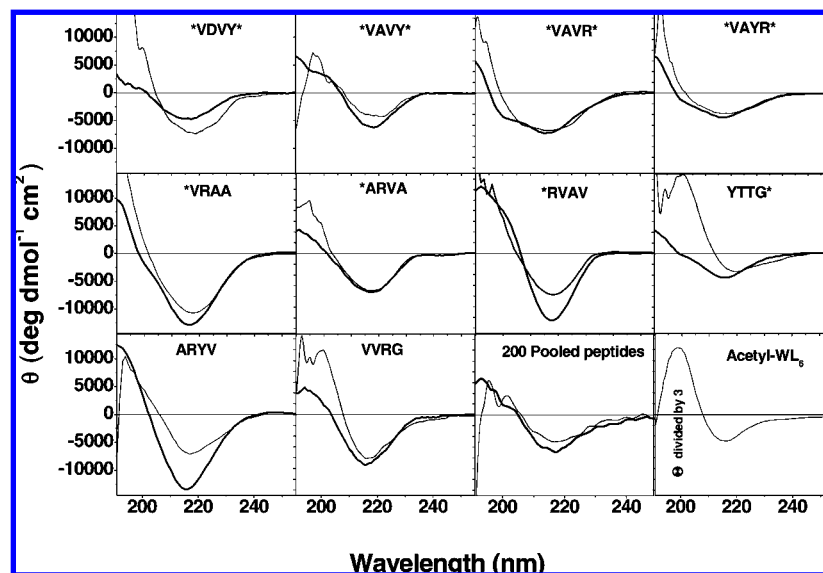


**Figure 5.** Secondary structure information obtained using CD spectra of the membrane-permeabilizing peptides. CD spectra were measured in phosphate buffer, pH 7.0, before (thick line) and after (thin line) addition of 2.5 mM phospholipid vesicles. The “pooled” peptide sample is an equimolar mixture of 200 randomly selected peptides from the library. The peptide in the lower right corner is the heptapeptide AcWL<sub>6</sub>, which forms highly ordered antiparallel  $\beta$ -sheets in bilayers.<sup>45,46</sup> The mean residue ellipticity for AcWL<sub>6</sub> has been divided by 3 to bring it onto the same scale as the other peptides. The spectra for the library peptides are given as mean residue ellipticities and indicate roughly 30%  $\beta$ -sheet content.

The libraries were designed with a potential dyad repeat that could favor  $\beta$ -strand structure, and their short length will disfavor helical structures, but the function-based selection criteria were not designed to select for any particular secondary structure. Circular dichroism spectroscopy (Figure 5) was used to examine the conformation of the soluble, membrane-destabilizing peptides (Figure 1). In phosphate buffer, most of the peptides had CD spectra with a weak negative band at  $\sim$ 218 nm and positive ellipticity around 200 nm, indicative of  $\beta$ -strand structure.<sup>44</sup> However, the molar ellipticities suggest a  $\beta$ -sheet content no greater than 25–30%. When 2.5 mM lipid vesicles are present, some of the peptides (e.g., YTTG\*) had increased  $\beta$ -sheet content, suggesting a slightly more ordered structure. Intramolecular  $\beta$ -sheet formation is unlikely in these peptides because of their short length, bulky aliphatic and aromatic residues, and lack of glycine or proline; therefore, we assume the  $\beta$ -sheets are intermolecular. The  $\beta$ -sheet content in buffer suggests that we are selecting for small water-soluble aggregates of peptides rather than monomeric peptides.

As a control, we also studied a pool of 200 peptides randomly selected from the library. Like the selected active peptides, the CD spectra of pooled peptides had some  $\beta$ -strand conformation in buffer. The fact that the pooled peptides bind to membranes and have secondary structure similar to that of the membrane-active peptides and yet do not permeabilize membranes (discussed below) indicates that these secondary structure features are present in the library design and were not a property that was strongly selected for in the screen.

For comparison, we also show the CD spectrum of the heptapeptide Acetyl-Trp-Leu<sub>6</sub>, which forms highly ordered, antiparallel  $\beta$ -sheets in membranes.<sup>45,46</sup> The molar ellipticity for AcWL<sub>6</sub>, which is nearly 100%  $\beta$ -sheet, has been divided

by 3 in Figure 5 to place it on the same scale as the library peptides, suggesting that the library peptides are not very highly ordered or highly organized, even when bound to lipid membranes. We have observed this behavior in other families of membrane-permeabilizing peptides, as well.<sup>7,9</sup>

**Peptide-Induced Leakage of Entrapped Contents from Vesicles.** The peptides selected from the library were synthesized, purified, and assayed for their ability to induce Tb<sup>3+</sup> leakage from 9:1 POPC:POPG LUVs in a concentration- and time-dependent manner. Detectable leakage was observed down to 1:500 P:L, a concentration range below that at which many natural membrane-permeabilizing peptides are active. The time dependence of Tb<sup>3+</sup> leakage showed that most of the selected peptides induce a rapid and transient leakage process within the first few minutes after peptide addition (Figure 6A). Within 10–15 min after peptide addition, the leakage from vesicles had ceased, except for peptides \*VDVY\* and \*VAYR\*, which have a slower overall time course. Nonetheless, the leakage induced by these two peptides also stops within about 30 min. Thus, for all peptides, leakage is a transient process that occurs after peptide addition and ceases with incomplete leakage (except at high peptide concentrations). A second addition of peptide caused a second burst of leakage (not shown). The random peptide pool did not cause any measurable Tb<sup>3+</sup> leakage at any P:L ratio studied, despite the fact that some members of the pool bind to vesicles and have  $\beta$ -sheet secondary structure.

The two peptides that caused unusually slow leakage were characterized in additional experiments to determine if the slow step was membrane binding, or if it was due to events that take place on the membrane after binding. As shown in Figure 6B, binding of these two peptides to vesicles is very rapid, occurring within a minute or so of addition, similar to the rapid binding of monomeric peptides.<sup>46,47</sup> All 10 of the active peptides bind with the same rapid kinetics (not shown). The slow time course of leakage for \*VDVY\* and \*VAVR\* must, therefore, be due

(44) Johnson, W. C. *Proteins* **1990**, *7*, 205–214.

(45) Bishop, C. M.; Walkenhorst, W. F.; Wimley, W. C. *J. Mol. Biol.* **2001**, *309*, 975–988.

(46) Wimley, W. C.; Hristova, K.; Ladokhin, A. S.; Silvestro, L.; Axelsen, P. H.; White, S. H. *J. Mol. Biol.* **1998**, *277*, 1091–1110.

(47) Pokorny, A.; Almeida, P. F. *Biochemistry* **2004**, *43*, 8846–8857.

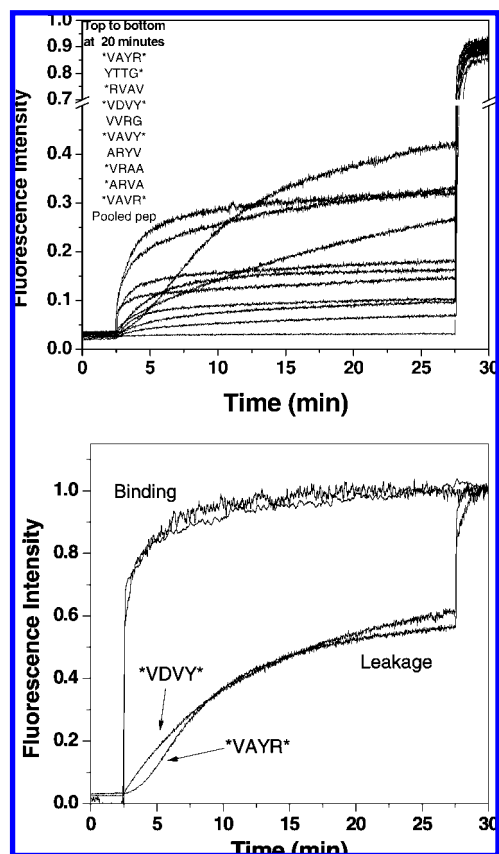


**Figure 6.** Peptide-induced leakage of  $\text{Tb}^{3+}$ /DPA from phospholipid vesicles. (A, top) Time course of leakage. Vesicles containing  $\text{Tb}^{3+}$  were first diluted into buffer containing an excess of DPA, and a baseline fluorescence intensity was established. At 2.5 min, peptide was added from a concentrated solution to achieve P:L = 1:200.  $\text{Tb}^{3+}$ /DPA complex formation gives rise to a fluorescence intensity that is measured. At 27.5 min, Triton X-100 was added to release all contents from the vesicles. Eight of the 10 peptides caused a rapid burst of leakage from the vesicle that was nearly complete within 10 min. Two of the peptides caused slower leakage, which was essentially complete by about 30 min. (B, bottom) Time dependence of binding and leakage. In this panel, we superimpose the time course of binding of the two unusually slow peptides, measured by tryptophan fluorescence, and the time course of leakage measured at P:L = 1:100.

to events that take place on the membrane after binding. Most interesting is the time course of \*VAYR\*, which shows a sigmoidal time course (i.e., with a lag phase). This is an unusual observation for membrane-permeabilizing peptides<sup>47</sup> and will be the subject of future mechanistic studies. For the purposes of this work, we note that the potency, general mechanism of action (below), and pore characteristics of all 10 peptides selected from the library using the premixing strategy are similar.

**Selectivity of Membrane Permeabilization.** The peptides were assayed for their ability to induce leakage of different fluorescent indicators from LUVs composed of 90% zwitterionic POPC and 10% anionic POPG. The  $\text{Tb}^{3+}$  leakage assay monitors the leakage of a zwitterionic citrate-chelated  $\text{Tb}^{3+}$  complex and the anionic weak acid DPA. The ANTS/DPX assay uses rigid, anionic and cationic ring compounds of about 425 g/mol. The diameters of these probes are 4–6 Å. We also used fluorescein-labeled dextrans of either 3000 or 40 000 g/mol which are ellipsoidal with a short axis of ~20 Å diameter.<sup>48</sup> Active

peptides induced significant leakage of the small-molecule indicators as well as some leakage of the 3000 Da dextran, but leakage of the 40 000 Da dextran was significantly lower (Table 2). Leakage of all probes occurs rapidly within the initial burst of leakage shown in Figure 6. Slow leakage of any of the probes at times longer than 1 h did not occur. These results show that, while there is not a strict size cutoff, the peptides can release molecules that are up to 20 Å in diameter with some selectivity based on size. This is consistent with observations made with other natural and synthetic membrane-destabilizing peptides.<sup>9,24</sup>

Leakage of contents from electrostatically neutral liposomes composed of 100% of the zwitterionic lipid POPC was also examined. We found that the pore-forming peptides, which are cationic and were selected using vesicles containing 10% of the anionic lipid POPG, also bind to and permeabilize zwitterionic vesicles (Table 2), although the efficiency of both processes is somewhat lower. Thus, electrostatic interactions with anionic lipids do not dominate the interaction of the peptides with the bilayers and are not required for binding or interfacial activity. This observation, which has now been made in several systems,<sup>7,9</sup> validates the design of our high-throughput screen, in which the 10 mol % concentration of anionic lipids is meant to modulate peptide interactions with bilayer but not dominate them.

**Mechanism of Pore Formation.** To explore the mechanism of the transient leakage, we employed the “requeenching” assay<sup>32</sup> in which the dye ANTS and the concentration-dependent quencher DPX are co-encapsulated within lipid vesicles. After leakage has taken place and has stopped, samples are titrated with external DPX to determine the fraction of ANTS that has leaked and the degree of quenching remaining inside the vesicles. This assay distinguishes between the two known mechanisms for transient, partial leakage from vesicles: “graded”, in which all the vesicles release a similar proportion of their contents, or “all-or-none”, in which a fraction of the vesicles release all of their contents while the remainder release none. Both mechanisms have been observed with membrane-active peptides in vesicles.<sup>9,24,33,49</sup> The results of the requeenching assay are shown in Figure 7 as a composite of the results for all 10 peptides, along with the expected behavior for graded versus all-or-none leakage. The selected membrane-permeabilizing peptides cause leakage by a predominantly all-or-none mechanism, even at very high fractional leakage. The implications of this observation are discussed below.

## Discussion

**Rational Combinatorial Design.** Peptides that bind to and permeabilize cell membranes are important in innate immunity and defense. However, despite an extensive literature and nearly a thousand known examples,<sup>50–52</sup> compelling structure–function relationships, rational design, or engineering successes in this field are rare, comprising only a few well-studied examples. Instead, recent literature, which is rich with studies on antimicrobial “pore-forming” peptides, suggests strongly that membrane-permeabilizing activity is often dependent not on specific amino

(48) Bohrer, M. P.; Deen, W. M.; Robertson, C. R.; Troy, J. L.; Brenner, B. M. *J. Gen. Physiol.* **1979**, *74*, 583–593.

(49) Hristova, K.; Selsted, M. E.; White, S. H. *J. Biol. Chem.* **1997**, *272*, 24224–24233.

(50) Fjell, C. D.; Hancock, R. E.; Cherkasov, A. *Bioinformatics.* **2007**, *23*, 1148–1155.

(51) Antimicrobial Peptides Database, <http://aps.unmc.edu/AP/main.html>.

(52) Antimicrobial Sequence Database, <http://www.bbcm.units.it/~tossi/amsdb.html>.



**Table 2.** Peptide-Induced Leakage (%) of Solute

	Tb <sup>3+</sup> /DPA leakage			Tb <sup>3+</sup> /DPA leakage			ANTS/DPX leakage			dextran leakage	
	90% POPC + 10% POPG			100% POPC			90% POPC + 10% POPG			3 kDa	40 kDa
peptide <sup>a</sup>	1:50 P:L	1:250 P:L	1:500 P:L	1:50 P:L	1:250 P:L	1:500 P:L	1:50 P:L	1:250 P:L	1:500 P:L	1:50 P:L	1:50 P:L
buffer	0	0	0	0	0	0	0	0	0	1	9
*VDVY*	74	19	6	56	1	1	91	31	6	44	2
*VAVY*	67	51	23	26	2	0	42	22	4	28	27
*VAVR*	65	15	7	7	0	0	83	34	20	25	5
*VAYR*	93	41	20	33	0	0	67	21	9	46	21
*VRAA	56	9	5	9	0	0	83	34	16	41	4
*ARVA	89	23	11	8	0	0	73	19	17	39	15
*RVAV	67	27	16	28	1	1	67	21	10	28	15
YTTG*	70	23	19	73	9	0	46	14	5	31	23
ARYV	81	18	6	43	5	1	75	29	15	44	19
VVRG	97	32	9	50	5	0	79	31	14	64	0
pool pep <sup>b</sup>	3	1	0	2	0	0	37	13	3	11	0
Triton-X <sup>c</sup>	100	100	100	100	100	100	100	100	100	100	100

<sup>a</sup> Complete peptide sequences are shown in Figure 1. Our notation shows the identity of the residues in the four varied positions, with asterisks denoting the presence of a terminal basic cassette. <sup>b</sup> The peptide pool was generated by extracting peptides from a pool of 200 randomly selected beads from the library. <sup>c</sup> Triton X-100 lyses all vesicles completely. All release values are based on fluorescence intensity 30–60 min after peptide-induced leakage divided by intensity after Triton X-100 solubilization.

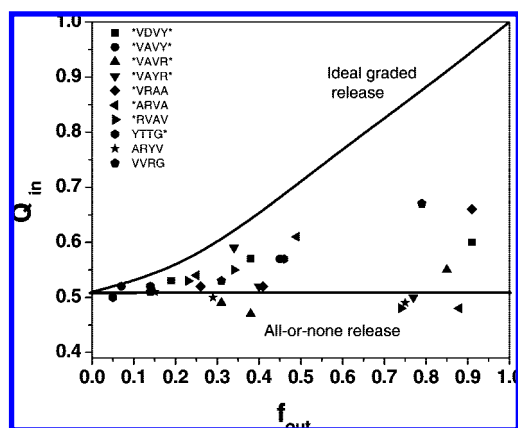


**Figure 7.** Requenching assay for determining the mechanism of contents leakage from lipid bilayer vesicles. Various concentrations of the 10 membrane-permeabilizing peptides were added to a constant vesicle solution with entrapped dye (ANTS) and quencher (DPX), as described in the text. After leakage had stopped (~30 min), the requenching assay<sup>32</sup> was used to determine the fraction of ANTS that had been released ( $f_{out}$ ) and the degree of quenching of the ANTS that remains entrapped within vesicles ( $Q_{in}$ ). Quenching is defined as a fractional fluorescence and thus ranges from ~0.5 (initial quenching level in these vesicle preparations) to 1 (unquenched). Theoretical curves for all-or-none and for graded release are shown. These peptides cause predominantly all-or-none release, in which a vesicle releases either all of its contents or none of them.

acid sequences or three-dimensional peptide structures but instead on a peptide's interfacial activity, which depends mainly on the appropriate balance of physical–chemical interactions between and among peptides, water, and membrane lipids. On the basis of these ideas, we have hypothesized that potent membrane-destabilizing peptides can be more effectively discovered by selection from libraries that vary a peptide's *composition* rather than libraries designed with a particular *structure* or *sequence* in mind or peptides designed or engineered rationally from known active sequences.

To test this hypothesis, we designed the 16 384-member combinatorial library of peptides shown in Figure 1. A functional, two-stage, high-throughput screen was used to detect contents leakage from lipid vesicles caused by peptides that are water-soluble, without regard to peptide structure or mechanism of action. We screened 20 000 library members and identified 14 soluble and very potent membrane-destabilizing peptides,

which are shown in Figure 2. Of the 14 identified sequences, three were identified multiple times independently (Figure 2). The observation of a Poisson distribution of identified sequences shows that there are only a very small number of soluble and highly potent membrane-permeabilizing peptides in the library and demonstrates that we have identified most of them. Despite the fact that we used a composition–space library with five of the nine core residues fixed, and despite the fact that the library contains many members that are very similar in sequence and secondary structure to the active peptides, the membrane-permeabilizing peptides that we identified are a unique and rare class in the library. Thus, we are describing a system with very high functional specificity and high stringency.

The selected sequences share a similar core hydrophobicity (Figure 3) and general compositional features, but they do not share a particular sequence motif, even a loosely defined one. Charged residues were found at least once in every varied core position. Active peptides had all possible lengths—9, 12, and 15 residues—with terminal basic cassettes (Figure 1) on both termini, on either terminus alone, or on neither terminus. Net charge ranged from +1 to +6. A strict dyad repeat<sup>34</sup> was not observed. Importantly, core sequences identified more than once in the screen were always found with the same termini ( $p = 0.004$ ), showing that that the terminal groups are a conserved part of a particular peptide's activity. Taken together, the observation that there is a rare and extraordinary group of potentially active sequences in the library and the observation that the potent peptides do not share a similar sequence motif or length support the idea that interfacial activity, which depends on physical–chemical interactions between peptide and lipid, is more important to function than specific peptide–peptide interaction or the formation of a specific three-dimensional structure. This idea is supported by the fact that all of the active peptides are only weakly structured in bilayers. We hypothesize that the rare, highly active peptides we have selected have the correct balance of solubility, hydrophobicity, amphipathicity, propensity to self-assemble into peptide–lipid domains, and ability to promote non-bilayer phases that leads to permeation.

**Mechanism of Peptide Activity.** Peptides that permeabilize membranes on the basis of their interfacial activity are expected to behave differently than peptides that assemble into long-lived water-filled channels across membranes. Such structures are the so-called “barrel stave” or “toroidal” peptide pores. We have

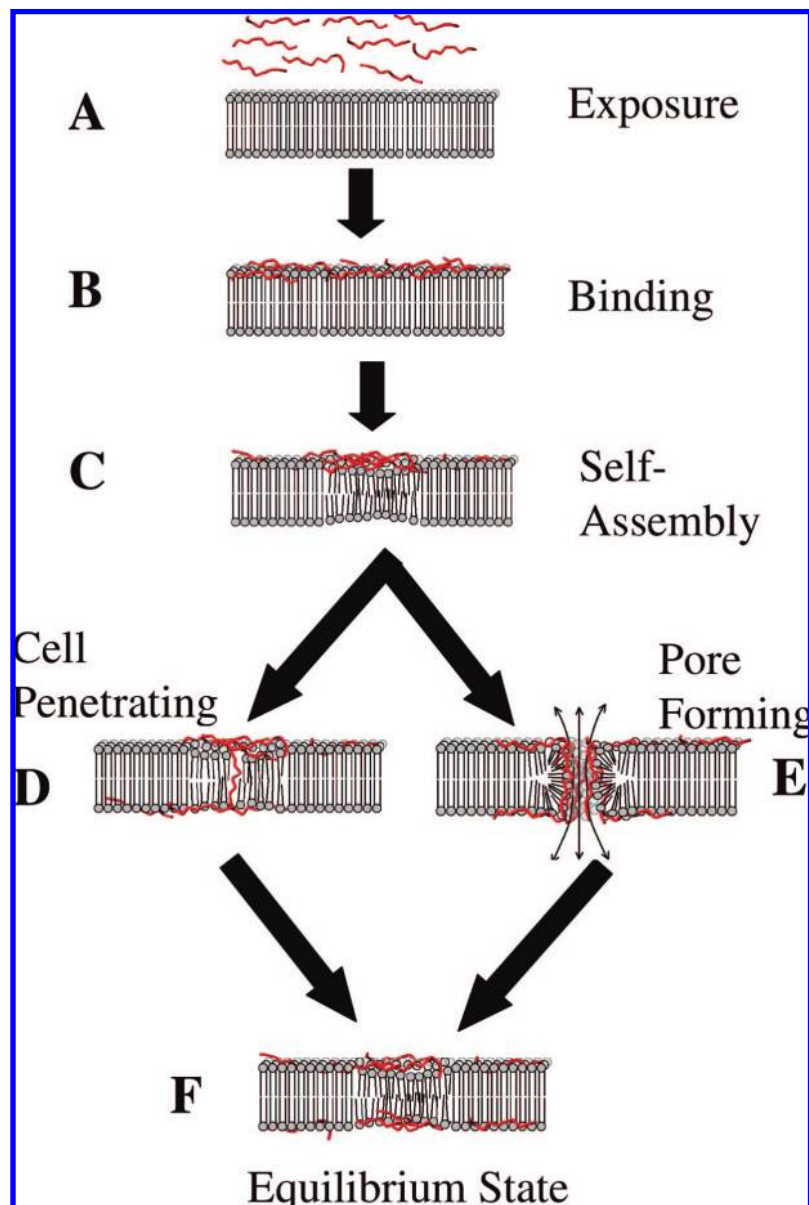


**Figure 8.** Enhanced mechanistic model for the actions of the pore-forming peptides in phospholipid bilayers. We propose that an amended “carpet” or “sinking raft” model of peptide pore formation explains our observations in the following steps. (A) Intact membranes are exposed to peptide. (B) Peptide binds to the outer monolayer due to hydrophobic and electrostatic interactions. (C) Peptides self-assemble into peptide–lipid domains in the outer monolayers. (D,E) Relief of the trans-bilayer asymmetry simultaneously through (D) a cell-penetrating peptide pathway that causes little or no leakage and (E) a cooperative pore formation that causes a vesicle to lose all of its entrapped contents. (F) The equilibrium state is reached, in which the transbilayer asymmetry has been fully dissipated and pore formation no longer occurs.

shown previously that a single water-filled, transmembrane pore in a vesicle would allow for the complete release of a vesicle’s contents in as little as 10 ms.<sup>24</sup> However, these types of pores as equilibrium structures have been observed only for a small number of soluble, membrane-permeabilizing peptides. For example, the well-studied pore-forming toxins alamethicin, from the fungus *Trichoderma viridae*, and melittin, from honey bee (*Apis mellifera*) venom, probably form long-lived transmembrane pores in at least some types of bilayers under some experimental conditions.<sup>53,54</sup>

Among the 1000 or so known membrane-permeabilizing peptides, such well-defined, trans-bilayer pores are the rare

exceptions, although specific pore structures are often assumed in structure–function studies. Instead, what is typically observed for natural membrane-active peptides in vesicles, and what we observe for the peptides identified in this work and in our previous work,<sup>7,9,24,33</sup> is the following: When peptides and vesicles are mixed at an active P:L ratio, a few hundred to a few thousand peptides bind rapidly (<1 min) to the outer monolayer of each lipid vesicle, resulting in a partial, transient burst of leakage of the vesicle contents, amounting to the release of a few hundred indicator molecules from each vesicle over the course of 5–30 min.<sup>55</sup> Except at the highest peptide concentrations, leakage stops or slows substantially before all the vesicle contents are released. These results are not consistent with a water-filled pore structure through the membrane, or any equilibrium pore structure, which would release all of the

(53) Huang, H. W.; Chen, F. Y.; Lee, M. T. *Phys. Rev. Lett.* **2004**, *92*, 198304.

(54) Qian, S.; Wang, W.; Yang, L.; Huang, H. W. *Biophys. J.* **2008**.

contents. Instead, many observations are consistent with transient, peptide-induced disturbances in the permeability barrier of the membrane, or perhaps a very short-lived, transient pore in a fraction of the vesicle population.

The key observation that must be explained by any proposed mechanism of action is why leakage from vesicles ceases, often with a half-time of only a few minutes, despite the fact that the peptides remain bound to the bilayers and have the same secondary structure. Furthermore, the moderate binding constants (Figure 4) and rapid on-rate for binding (Figure 6B) mean that peptides will rapidly equilibrate between vesicles. This type of mechanism is exemplified by the “carpet model” or “sinking raft” models of peptide permeabilization of membranes,<sup>5,47</sup> which explain transient leakage by positing four stages of membrane permeabilization, as shown in Figure 8: (1) initial surface binding, in which monomeric peptides bind to the outer monolayer due to hydrophobic and electrostatic interactions; (2) self-assembly of the peptides into peptide-rich domains on the outer monolayer, creating an imbalance of mass, charge, or surface tension across the bilayer; (3) formation of transient nonbilayer structures that relieve the imbalance across the bilayer by allowing trans-bilayer equilibration of peptide and lipid as well as release of entrapped contents; and finally, (4) the equilibrium stage in which the asymmetry-driven trans-bilayer movement, and concomitant leakage, no longer occur because the peptide is equilibrated across the membrane. Almeida and colleagues have even suggested that transient membrane destabilization and leakage could occur without peptide self-assembly.<sup>47,56</sup>

**A New Model.** The peptides we have described here cause leakage from membrane vesicles by an all-or-none mechanism, which is nonetheless transient and partial at most peptide concentrations. Because the vesicles are uniform<sup>57</sup> and every vesicle has hundreds of peptides initially bound to it, this observation means that those vesicles that do not leak their contents must achieve transbilayer equilibrium of peptide (Figure 8) by a mechanism that does not invoke leakage. Thus, there are at least two paths by which peptides can cross the membranes to relieve the asymmetry that occurs when they initially bind: a stochastic, “catastrophic” pore event<sup>58</sup> that causes a vesicle to release all of its contents, and a second pathway that does not cause leakage. During the transient leakage phase of an experiment, we assume that both processes are relieving the trans-bilayer peptide asymmetry simultaneously (Figure 8); therefore, the probability of a pore event decreases with time until it reaches zero. Because the leakage is likely to be a cooperative event, it is reasonable for it become more probable with increasing peptide concentration, as we observed. This model is consistent with the hypothesized overlap in mechanism between pore-forming peptides, which cross a

membrane and cause leakage, and cell-penetrating peptides, which cross membranes without causing leakage.<sup>59</sup>

Our data also provide some information about the nature of the transient “pore” state. There is a weak distinction based on the size and charge of the probe molecule being released. Between the small molecules ANTS/DPX (~425 g/mol) and Tb<sup>3+</sup>/DPA (100–150 g/mol), the first pair sometimes leaks to a greater extent (Table 2) despite their larger molecular weight, suggesting a distinction based on charge distribution, hydrophobicity, or molecular shape in addition to molecular size. We have observed the same relative difference for other families of pore-forming peptides.<sup>9</sup> A dextran molecule of 3000 Da is released readily, while a 40 000 Da dextran is not released as effectively. These data provide an image of a pore that can release molecules up to about 20 Å in diameter but is also sensitive to size and charge of molecules that are only 150–425 Da, suggesting a “pore state” that is not a simple water-filled pore but instead a complex, transient non-bilayer phase containing peptides, lipids, water, and polar solutes.

## Conclusion

We have designed a narrow, compositionally varied combinatorial peptide library to select soluble, membrane-permeabilizing peptides by a two-step, function-based high-throughput screen. The peptides identified are small and soluble, but they also bind to bilayer membranes and induce membrane permeabilization at low peptide concentration. We describe here the amino acid sequences and mechanism of action of the rare, potent pore-formers selected from this library. Although they share little sequence similarity in variable positions, the most active molecules share physical properties such as core hydrophobicity, and they share the same secondary structure and mechanism of action. The observed mechanism is consistent with nonspecific “interfacial activity” being the critical factor leading to potent membrane-destabilizing activity. We showed here that only about 1 in 1000 peptides in the library had the requisite activity, despite the library being narrowly defined. This “interfacial activity” is a complex function of a peptide’s hydrophobicity, amphipathicity, and propensity to self-assemble into peptide-rich domains, coupled with potential for it to alter the packing and curvature of the lipids such that non-bilayer phases are promoted (Figure 8). While one can describe these factors individually with some degree of certainty, rational engineering of such complex interfacial activity is not possible. This idea is strengthened by the fact that the library contains many peptides that are very similar to the active peptides and yet were not selected. We demonstrate here that composition–space peptide libraries coupled with function-based high-throughput screens can lead to the discovery of diverse, soluble, and highly potent interfacially active peptides.

**Acknowledgment.** This work is supported by NIH grant GM60000 and a Louisiana Board of Regents RC/EEP grant. The authors acknowledge Christopher M. Bishop for peptide synthesis and purification. We sincerely thank Drs. Kalina Hristova, Paulo F. Almeida, and Mikhail Merzliakov for enlightening discussions and/or for critically reading the manuscript.

JA8017863

(55) A large unilamellar vesicle of 0.1 μm diameter has about 100 000 lipid molecules and has an internal volume of about 10<sup>-19</sup> L. Thus, an experiment at P:L = 250 and 10 mM entrapped solute will have ~400 bound peptides and ~600 probe molecules entrapped in each vesicle.

(56) Yandek, L. E.; Pokorny, A.; Floren, A.; Knoelke, K.; Langel, U.; Almeida, P. F. *Biophys. J.* **2007**, *92*, 2434–2444.

(57) Mayer, L. D.; Hope, M. J.; Cullis, P. R. *Biochim. Biophys. Acta* **1986**, *858*, 161.

(58) Gregory, S. M.; Cavanaugh, A.; Journigan, V.; Pokorny, A.; Almeida, P. F. *Biophys. J.* **2008**, *94*, 1667–1680.

(59) To further test this correlation, we are currently screening composition-based libraries for “cell-penetrating peptides” which can cross bilayers without causing leakage.